STATISTICS OF NORMALLY DISTRIBUTED INITIAL IMPERFECTIONS†

KIYOHIRO IKEDA

Department of Civil Engineering, Tohoku University, Aoba, Sendai 980, Japan

and

KAZUO MUROTA

Research Institute for Mathematical Sciences, Kyoto University, Kyoto 606, Japan

Abstract—This paper offers a theoretical study on the probabilistic nature of critical loads (buckling loads) of structures subject to normally distributed initial imperfections. Explicit form of probability density function of critical loads are derived for various types of critical points. Double bifurcation points of structures with regular-polygonal symmetry are dealt with by means of the group-theoretic bifurcation theory. The distribution of minimum values of the critical loads is investigated to present a statistical design index. The theoretical and empirical probability density functions for simple structures are compared to show the validity and effectiveness of this method. The method is quite efficient when it is directly applicable; otherwise, the explicit forms, at least, can greatly supplement the inefficiency of the conventional random method.

1. INTRODUCTION

Initial imperfections of members and of materials of structures make their critical loads (buckling loads) essentially uncertain and indeterministic. The method of random initial imperfections with known probabilistic properties, which obtains these loads numerically or experimentally for a number of random initial imperfections, would reflect their probabilistic nature [see e.g. Elishakoff (1979, 1983), Elishakoff and Arbocz (1982), Elishakoff *et al.* (1987), Lindberg (1988), Kirkpatrick and Holmes (1989), and Arbocz and Hol (1991)]. The stochastic finite-element method has been developed to incorporate the random properties of structures and soils in analysis [see e.g. Astill *et al.* (1972) and Baecher and Ingra (1981)].

The imperfection sensitivity laws by Koiter (1945) deterministically relate critical load to imperfection magnitude for a given mode of imperfection when the magnitude is infinitesimally small. Roorda and Hansen (1972) extended these laws to a single mode normally-distributed initial imperfection and successfully arrived at failure probabilities, without resort to the asymptoticity assumption of imperfection magnitude. Elishakoff *et al.* (1987), following the pioneering work of Bolotin (1958), extended these laws to multimode initial imperfections subject to multivariate normal distributions to obtain reliability curves with reference to experimental samples. Arbocz and Hol (1991) utilized measured initial imperfections of axially compressed cylindrical shells to evaluate the statistical nature of their critical loads with the use of the first-order, second-moment method [*cf.* Karadeniz *et al.* (1982)].

In order to develop a potential design alternative, which can efficiently implement a stochastic viewpoint, the authors have presented a series of asymptotic theories on initial imperfections by extending the Koiter laws. Here the word asymptotic indicates that the results hold accurately for an (infinitesimally) small imperfection magnitude and in a sufficiently close neighborhood of the critical point. At the expense of the asymptoticity assumption, the results obtained have become quite general and simple, thus achieving a deeper insight, as was the case with the Koiter laws. The critical initial imperfection vector, which achieves the steepest decline of critical load under the constraint of a constant norm, was explicitly obtained in Ikeda and Murota (1990a) for various kinds of simple critical

---

† Part of this paper has been presented in the Second Japan-Korea Joint Seminar on Steel Bridges, July 1992.

points, and in Murota and Ikeda (1991) for group-theoretic double points, which appear generically for (dome and shell) structures with regular-polygonal symmetry. The bifurcation equation, which characterizes relevant bifurcation behavior, was derived by expanding the equilibrium equations into power series in the vicinity of the critical point, and by eliminating the passive coordinates. This process of deriving the bifurcation equation is called the Lyapunov–Schmidt–Koiter decomposition [see e.g. Sattinger (1979), Golubitsky and Schaeffer (1985), and Golubitsky et al. (1988)]. Then from this equation the explicit form of the critical load reduction, and, in turn, that of the critical initial imperfection vector are obtained in an asymptotic sense. In particular, for the double points, the so-called group-theoretic approach in bifurcation theory is vital in the investigation of the vanishing or nonvanishing of the terms in the equation [see e.g. Sattinger (1979), Golubitsky and Schaeffer (1985), Golubitsky et al. (1988), Healey (1988), and Dinkevich (1991) for mathematical backgrounds. See also Ikeda et al. (1991), and Murota and Ikeda (1991, 1992) for an exposition of its application to structures].

These studies for the critical imperfection revealed that the space of imperfection vectors is to be divided into two orthogonal subspaces: the subspace that affects the critical load and the other that does not. The former subspace is spanned by the critical imperfection vector(s). Based on this result, when an initial imperfection vector is assumed to be randomly distributed under the constraint of a constant norm, explicit forms of the probability density function of critical loads have been obtained in Ikeda and Murota (1991) for simple points, and in Murota and Ikeda (1992) for the double ones. The knowledge of these forms, which yield various statistical properties, such as the expected value and the variance, of the critical loads is quite comprehensive and is expected to be of great assistance in design. Such an assumption on the distribution, however, is suited for the theoretical derivation but is not very realistic in that the norm in general changes randomly.

In order to address this problem, we present a theoretical method on normally distributed initial imperfections. Asymptotically the increment of the critical loads for the critical points can be expressed as a function in one or two variables (according to whether the point is simple or double), which is (are) also subject to a normal distribution. This makes it possible for various types of critical points to derive the probability density function and relevant stochastic properties of the critical loads. Explicit formulae for reliability functions are presented for some of the critical points, while the integral forms of the functions are applicable for the remaining ones. In addition, in order to reduce an analytical task we present a semi-empirical evaluation procedure which obtains this function with reference to the sample mean and the sample variance of critical loads observed in an experiment or an analysis. The distribution of the minimum values of the critical loads is investigated with the hope of providing a design index based on a firm statistical theory. The present method is applied to simple example structures to show its usefulness.

2. FORMULATION

This section offers the formulation of the present problem, due to Murota and Ikeda (1992), which is applicable both to simple and double critical points. We consider a system of nonlinear equilibrium equations

$$H(\lambda, u, v) = o, \tag{1}$$

where λ denotes a loading parameter; u indicates an N-dimensional nodal displacement (or position) vector; and v a p-dimensional imperfection pattern vector. We assume H to be sufficiently smooth (or even analytic) and that the eigenvalues of the tangent stiffness (Jacobian) matrix

$$J = J(\lambda, u, v) = (J_{ij}) = \left(\frac{\partial H_i}{\partial u_j}\right)$$

of H for the perfect system are all positive at the initial state $(\lambda, u) = (0, o)$. This means that the system is originally (subcritically) in a stable state.

For a fixed $\mathbf{v}$, a set of solutions $(\lambda, \mathbf{u})$ of the above system of equations makes up equilibrium paths. Let $(\lambda_c, \mathbf{u}_c) = (\lambda_c(\mathbf{v}), \mathbf{u}_c(\mathbf{v}))$ denote the first critical point on the main path of engineering interest $[(\cdot)_c$ refers to the critical point], governing the critical load (buckling load) of the structure with an imperfection pattern vector $\mathbf{v}$. The tangent stiffness matrix is singular at $(\lambda_c, \mathbf{u}_c, \mathbf{v})$:

$$\det [J(\lambda_c, \mathbf{u}_c, \mathbf{v})] = 0. \tag{2}$$

In particular, this is satisfied by the critical point $(\lambda_c^0, \mathbf{u}_c^0, \mathbf{v}^0)$ of the perfect system $[(\cdot)^0$ refers to the perfect system]. It is assumed that we can choose $\boldsymbol{\xi}_i$ $(i = 1, \ldots, M)$ to be M critical eigenvectors of J^0 such that

$$\boldsymbol{\xi}_i^{\mathrm{T}} \boldsymbol{\xi}_j = \delta_{ij}, \quad i, j = 1, \ldots, M,$$

$$\boldsymbol{\xi}_i^{\mathrm{T}} J^0 = \mathbf{o}^{\mathrm{T}}, \quad i = 1, \ldots, M,$$

where M is the multiplicity of the critical point and δ_{ij} is the Kronecker delta. Define by

$$P = \sum_{i=1}^{M} \boldsymbol{\xi}_i \boldsymbol{\xi}_i^{\mathrm{T}} \tag{3}$$

the orthogonal projection matrix onto $\ker((J^0)^{\mathrm{T}})$, which characterizes the influence of initial imperfections.

We write

$$\mathbf{v} = \mathbf{v}^0 + \varepsilon \mathbf{d}$$

and

$$\lambda_c = \lambda_c^0 + \tilde{\lambda}_c, \tag{4}$$

where $\varepsilon(>0)$ denotes the magnitude of the initial imperfection; $\tilde{\lambda}_c$ means the increment of the critical load; and

$$\mathbf{d} = (d_1, \ldots, d_p)^{\mathrm{T}}$$

indicates its pattern (normalized in an appropriate way).

We are interested in the stochastic behavior of the critical load λ_c for random imperfections $\mathbf{v}$. To be more specific, we consider the case where the imperfection magnitude ε is small and where the imperfection mode $\mathbf{d}$ is subject to a multivariate normal distribution $N(\mathbf{o}, W^{-1})$. Here $N(\mathbf{c}, W^{-1})$ denotes the normal distribution with a mean $\mathbf{c}$ and a variance-covariance characterized by a positive definite matrix W^{-1}. The theoretical development will be continued in Section 3 (for simple points) and in Section 4 (for double points). The analyses are asymptotic in the sense that they are valid only when ε is small.

As we will see later, the imperfection sensitivity matrix defined by

$$B = (B_{ij}) = \left(\frac{\partial H_i}{\partial v_j} \bigg|_{(\lambda, \mathbf{u}, \mathbf{v}) = (\lambda_c^0, \mathbf{u}_c^0, \mathbf{v}^0)} \bigg| i = 1, \ldots, N; j = 1, \ldots, p \right) \tag{5}$$

plays the primary role in evaluating the influence of $\mathbf{d}$ on the critical load. For truss structures the explicit forms of the matrix B for various kinds of imperfection variables have already been obtained in Ikeda and Murota (1990b).

3. THEORY FOR SIMPLE CRITICAL POINTS

An asymptotic theory for normally distributed initial imperfections, valid in the neighborhood of a simple critical point of the perfect system, is presented in this section. This

serves as an extension of Ikeda and Murota (1991) for initial imperfections uniformly distributed on a sphere of $\|\mathbf{d}\|$ = constant. The explicit form of probability density function and relevant statistical properties are derived in order to reveal the stochastic nature of critical loads.

As has been made clear in Murota and Ikeda (1991), the asymptotic behavior of the increment (increase or decrease) $\tilde{\lambda}_c$ of the critical load λ_c of the imperfect system for simple critical points (and also for double ones to be dealt with in Section 4) is known to be expressed as

$$\tilde{\lambda}_c = \lambda_c - \lambda_c^0 \sim C(\mathbf{d})\varepsilon^\rho \tag{6}$$

when ε is small. The increment $\tilde{\lambda}_c$ is characterized by the exponent ρ and the coefficient $C(\mathbf{d})$, the explicit forms of which for simple critical points are given as follows† [cf. Koiter (1945) and Ikeda and Murota (1990a)]:

$$\begin{cases} \rho = 1, & C(\mathbf{d}) = -C_0 a & \text{at limit point,} \\ \rho = 1/2, & C(\mathbf{d}) = -C_0|a|^{1/2} & \text{at asymmetric bifurcation point,} \\ \rho = 2/3, & C(\mathbf{d}) = -C_0 \cdot a^{2/3} & \text{at unstable-symmetric bifurcation point,} \\ \rho = 2/3, & C(\mathbf{d}) = C_0 \cdot a^{2/3} & \text{at stable-symmetric bifurcation point.} \end{cases} \tag{7}$$

Here C_0 are positive constants, and the coefficients $C(\mathbf{d})$ depend on $\mathbf{d}$ through one variable

$$a \equiv \boldsymbol{\xi}^{\mathrm{T}} B \mathbf{d} = \sum_{i=1}^{p} c_i d_i, \tag{8}$$

where $\boldsymbol{\xi} = \boldsymbol{\xi}_1$; and

$$(c_1, \ldots, c_p)^{\mathrm{T}} = B^{\mathrm{T}}\boldsymbol{\xi}.$$

Since the increment $\tilde{\lambda}_c$ in eqn (6) for the stable point corresponds to the limit point for the secondary imperfect path, which does not have physical meaning, we hereafter exclude this point.

Denote by $f_{d_i}(d_i)$ the probability density function of $d_i (i = 1, \ldots, p)$. Then by eqn (8) the probability density function of a is given as the convolution integral of the scaled $f_{d_i}(d_i)$ $(i = 1, \ldots, p)$. This convolution could be computed via the Fourier transformation. Then a simple transformation from a to the critical load λ_c, through eqns (6) and (7), yields the probability density function of λ_c as we will see later. It is also remarked that the central limit theorem (Kendall and Stuart, 1977) says that under fairly mild conditions we may regard a as being normally distributed when p is large.

3.1. Stochastic properties of the critical load

An asymptotic theory for initial imperfections $\varepsilon\mathbf{d}$ subject to the normal distribution $N(\mathbf{o}, \varepsilon^2 W^{-1})$ is presented in this subsection. The variable a of eqn (8), which is a sum of normally-distributed variables $c_i d_i$ $(i = 1, \ldots, p)$, is subject to a normal distribution $N(0, \tilde{\sigma}^2)$ with mean 0 and variance

$$\tilde{\sigma}^2 = \boldsymbol{\xi}^{\mathrm{T}} BW^{-1}B^{\mathrm{T}}\boldsymbol{\xi}. \tag{9}$$

A normalized variable

---

† It is to be noted that for the asymmetric bifurcation point the increment $\tilde{\lambda}_c$ in eqn (6), and hence all the results in this section, has been defined as the conditional distribution given that a limit point exists on the primary branch of the imperfect system.

$$\tilde{a} = \frac{a}{\tilde{\sigma}}$$

is subject to the standard normal distribution $N(0, 1)$; the probability density function of $\tilde{a}$ is expressed as:

$$f_{\tilde{a}}(\tilde{a}) = \frac{1}{\sqrt{2\pi}} \exp\left(\frac{-\tilde{a}^2}{2}\right).$$

We introduce a normalized critical load (increment)

$$\zeta = \frac{\tilde{\lambda}_c}{C_0 \sigma^\rho} = \begin{cases} -\tilde{a} & \text{at limit point } (\rho = 1), \\ -|\tilde{a}|^{1/2} & \text{at asymmetric bifurcation point } (\rho = 1/2), \\ -\tilde{a}^{2/3} & \text{at unstable-symmetric bifurcation point } (\rho = 2/3), \end{cases} \tag{10}$$

where

$$\sigma = \tilde{\sigma}\varepsilon = (\xi^T B W^{-1} B^T \xi)^{1/2} \varepsilon \tag{11}$$

by eqn (9). Then the formula

$$f_\zeta(\zeta) = \begin{cases} f_{\tilde{a}}(\tilde{a}) \, d\tilde{a}/d\zeta, & -\infty < \zeta < \infty & \text{at limit point,} \\ 2f_{\tilde{a}}(\tilde{a}) \, d\tilde{a}/d\zeta, & -\infty < \zeta < 0 & \text{at asymmetric bifurcation point,} \\ 2f_{\tilde{a}}(\tilde{a}) \, d\tilde{a}/d\zeta, & -\infty < \zeta < 0 & \text{at unstable-symmetric bifurcation point} \end{cases} \tag{12}$$

yields the probability density function of ζ. Then the cumulative distribution function $F_\zeta(\zeta)$ of ζ is obtained by

$$F_\zeta(\zeta) = \int_{-\infty}^\zeta f_\zeta(\zeta) \, d\zeta, \tag{13}$$

and, in turn, the reliability function $R_\zeta(\zeta)$ of ζ is evaluated by:

$$R_\zeta(\zeta) = 1 - F_\zeta(\zeta), \tag{14}$$

which stands for the probability of failure, that is, that of the critical load exceeding the designed one. From eqns (12), (13) and (14) we obtained $f_\zeta(\zeta)$, $R_\zeta(\zeta)$, the expected value $E[\zeta]$, and the variance $\text{Var}[\zeta]$, for various kinds of simple critical points as below, where $\Gamma(\cdot)$ denotes the gamma function and

$$\Phi(\zeta) = \int_{-\infty}^\zeta \frac{1}{\sqrt{2\pi}} \exp\left(\frac{-\zeta^2}{2}\right) d\zeta$$

indicates the error function.

Limit point:

$$f_\zeta(\zeta) = \frac{1}{\sqrt{2\pi}} \exp\left(\frac{-\zeta^2}{2}\right), \quad -\infty < \zeta < \infty \quad \text{(standard normal distribution } N(0, 1)), \tag{15}$$

$$R_\zeta(\zeta) = 1 - \Phi(\zeta), \tag{16}$$

$$E[\zeta] = 0,$$

$$E[|\zeta|] = \frac{2}{\sqrt{2\pi}},$$

$$\mathrm{Var}\,[\zeta] = E[\zeta^2] = 1.$$

Asymmetric point of bifurcation (*conditional on the existence of a limit point*) :

$$f_\zeta(\zeta) = \frac{4|\zeta|}{\sqrt{2\pi}} \exp\left(\frac{-\zeta^4}{2}\right), \quad -\infty < \zeta < 0, \tag{17}$$

$$R_\zeta(\zeta) = 1 - 2\Phi(-\zeta^2), \tag{18}$$

$$E[\zeta] = \frac{-2^{3/4}}{\sqrt{2\pi}}\Gamma\left(\frac{3}{4}\right) = -0.822,$$

$$E[\zeta^2] = \frac{2}{\sqrt{2\pi}},$$

$$\mathrm{Var}\,[\zeta] = (0.349)^2.$$

Unstable-symmetric point of bifurcation :

$$f_\zeta(\zeta) = \frac{3|\zeta|^{1/2}}{\sqrt{2\pi}} \exp\left(\frac{-|\zeta|^3}{2}\right), \quad -\infty < \zeta < 0, \tag{19}$$

$$R_\zeta(\zeta) = 1 - 2\Phi(-|\zeta|^{3/2}), \tag{20}$$

$$E[\zeta] = \frac{-2^{5/6}}{\sqrt{2\pi}}\Gamma\left(\frac{5}{6}\right) = -0.802,$$

$$E[\zeta^2] = \frac{2^{7/6}}{\sqrt{2\pi}}\Gamma\left(\frac{7}{6}\right) = 0.831,$$

$$\mathrm{Var}\,[\zeta] = (0.432)^2.$$

The probability density functions $f_\zeta(\zeta)$ and the reliability functions $R_\zeta(\zeta)$ of these three types of critical points are plotted in Figs 1(a) and (b), respectively. Note that $\zeta = 0$
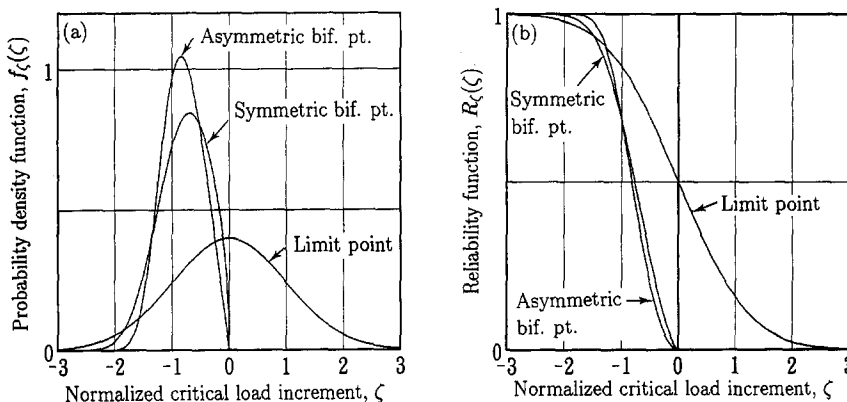

Fig. 1. Probability density functions $f_\zeta(\zeta)$ and reliability functions $R_\zeta(\zeta)$ of normalized critical load increment ζ for various types of simple critical points. (a) Probability density functions. (b) Reliability functions.

corresponds to the critical load $\lambda = \lambda_c^0$ for the perfect structure, and for bifurcation points the reliability of the structure is nullified at $\zeta = 0$ ($R_\zeta(0) = 0$). For the appropriately normalized critical load ζ, its probability density function $f_\zeta(\zeta)$ is independent of individual structures and is unique for each type of critical point. Details of structures, such as stiffness distribution, geometrical configuration, material property, and so on, do not affect the form of this function but the values of λ_c^0 and $C_0\sigma^p$.

The probability density function of the critical load λ_c is evaluated to be

$$f_{\lambda_c}(\lambda_c) = \begin{cases} g_1(\lambda_c), & -\infty < \lambda_c < \infty & \text{at limit point,} \\ 2g_{1/2}(\lambda_c), & -\infty < \lambda_c < \lambda_c^0 & \text{at asymmetric bifurcation point,} \\ 2g_{2/3}(\lambda_c), & -\infty < \lambda_c < \lambda_c^0 & \text{at unstable-symmetric bifurcation point,} \end{cases} \tag{21}$$

where

$$g_\rho(\lambda_c) = \frac{|\lambda_c - \lambda_c^0|^{1/\rho - 1}}{\sqrt{2\pi}\rho(C_0\sigma^\rho)^{1/\rho}} \exp\left(\frac{-1}{2}\left|\frac{\lambda_c - \lambda_c^0}{C_0\sigma^\rho}\right|^{2/\rho}\right). \tag{22}$$

The mean $E[\lambda_c]$ of λ_c is computed as

$$E[\lambda_c] = \lambda_c^0 + E[\zeta]C_0\sigma^\rho$$

$$= \begin{cases} \lambda_c^0 & \text{at limit point,} \\ \lambda_c^0 - 0.822C_0\sigma^{1/2} & \text{at asymmetric bifurcation point,} \\ \lambda_c^0 - 0.802C_0\sigma^{2/3} & \text{at unstable-symmetric bifurcation point,} \end{cases} \tag{23}$$

and the variance $\text{Var}\,[\lambda_c]$ of λ_c as

$$\text{Var}\,[\lambda_c] = \text{Var}\,[\zeta](C_0\sigma^\rho)^2$$

$$= \begin{cases} (C_0\sigma)^2 & \text{at limit point,} \\ (0.349C_0\sigma^{1/2})^2 & \text{at asymmetric bifurcation point,} \\ (0.432C_0\sigma^{2/3})^2 & \text{at unstable-symmetric bifurcation point.} \end{cases} \tag{24}$$

From eqns (16), (18) and (20), the reliability function of the critical load λ_c becomes

$$R_{\lambda_c}(\lambda_c) =$$

$$\begin{cases} 1 - \Phi\left(\frac{\lambda_c - \lambda_c^0}{C_0\sigma}\right) & -\infty < \lambda_c < \infty & \text{at limit point,} \\ 1 - 2\Phi\left(-\left(\frac{\lambda_c - \lambda_c^0}{C_0\sigma^{1/2}}\right)^2\right) & -\infty < \lambda_c < \lambda_c^0 & \text{at asymmetric bifurcation point,} \\ 1 - 2\Phi\left(-\left|\frac{\lambda_c - \lambda_c^0}{C_0\sigma^{2/3}}\right|^{3/2}\right) & -\infty < \lambda_c < \lambda_c^0 & \text{at unstable-symmetric bifurcation point.} \end{cases}$$

3.2. Evaluation of probability density function

We here present theoretical and semi-empirical evaluation procedures for the parameter $C_0\sigma^2$ in eqns (10) and (22) defining the probability density function, while the conventional way to obtain the histogram based on random initial imperfections is called the empirical evaluation.

The theoretical one is applicable when the equilibrium equations (1) can be differentiated to arrive at the imperfection sensitivity matrix B in eqn (5). Such a differentiation can be carried out for each element to obtain element matrices for B, and these matrices are assembled for the whole structure to obtain B, in compatibility with the framework of finite element analysis [see Ikeda and Murota (1990b) for its application to trusses]. Then

eqn (11) yields σ^2; C_0 is evaluated with reference to eqns (6) and (7) by obtaining the critical load λ_c from eqns (1) for a given imperfection mode **d**. Thus the theoretical evaluation of the probability density function is quite simple and straightforward.

The semi-empirical evaluation procedure is suggested for use when B cannot be computed, as is usually the case with experiments and highly nonlinear analyses. In this regard this procedure will be quite suited for practical use. For a series of random imperfection modes **d** chosen based on a known normal distribution, critical loads λ_c of a structure are evaluated by solving eqns (1). Then the sample mean $E_{\text{sample}}[\lambda_c]$ and the sample variance $\text{Var}_{\text{sample}}[\lambda_c]$ are computed based on random λ_cs computed in this manner. The critical load λ_c^0 for the perfect system and the variable $C_0\sigma^\rho$ are computed from eqns (23) and (24) as

$$C_0\sigma^\rho = \begin{cases} (\text{Var}_{\text{sample}}[\lambda_c])^{1/2} & \text{at limit point } (\rho = 1), \\ (\text{Var}_{\text{sample}}[\lambda_c])^{1/2}/0.349 & \text{at asymmetric bifurcation point } (\rho = 1/2), \\ (\text{Var}_{\text{sample}}[\lambda_c])^{1/2}/0.432 & \text{at unstable-symmetric bifurcation point } (\rho = 2/3), \end{cases} \tag{25}$$

$$\lambda_c^0 = \begin{cases} E_{\text{sample}}[\lambda_c] & \text{at limit point}, \\ E_{\text{sample}}[\lambda_c] + 2.35\,(\text{Var}_{\text{sample}}[\lambda_c])^{1/2} & \text{at asymmetric bifurcation point}, \\ E_{\text{sample}}[\lambda_c] + 1.86\,(\text{Var}_{\text{sample}}[\lambda_c])^{1/2} & \text{at unstable-symmetric bifurcation point}. \end{cases} \tag{26}$$

The substitution of the values of $C_0\sigma^\rho$ and λ_c^0 into eqns (21) and (22) leads to the semi-empirical probability density function $f_{\lambda_c}(\lambda_c)$ of critical load λ_c.

3.3. Distribution of minimum values

In this section we show that the minimum critical load achieved by a series of random imperfections **d** will serve as an index of extreme values. Such an index will be of great assistance in developing a sound designing procedure based on a firm statistical standpoint.

Let ζ_K be the minimum value of the normalized critical load ζ of eqn (10) attained by K independent random imperfections. The asymptotic form of the cumulative distribution function $F_K(\zeta_K)$ of ζ_K (as $K \to +\infty$) can be derived as [see Theorem 2.1.6 of Galambos (1978); also Kendall and Stuart (1977)]

$$\lim_{K \to \infty} F_K(c_K + d_K x) = \lim_{K \to \infty} \Pr\{\zeta_K \leqslant c_K + d_K x\} = 1 - \exp(-e^x) \tag{27}$$

with

$$c_K = \begin{cases} -(2\log K)^{1/2}\left[1 - \dfrac{\log\log K + \log(4\pi)}{4\log K}\right] & \text{at limit point}, \\[3ex] -[2\log(2K)]^{1/4}\left[1 - \dfrac{\log\log(2K) + \log(4\pi)}{4\log(2K)}\right]^{1/2} & \text{at asymmetric bifurcation point}, \\[3ex] -[2\log(2K)]^{1/3}\left[1 - \dfrac{\log\log(2K) + \log(4\pi)}{4\log(2K)}\right]^{2/3} & \text{at unstable-symmetric bifurcation point}, \end{cases}$$

$$d_K = \begin{cases} (2\log K)^{-1/2} & \text{at limit point}, \\ \tfrac{1}{2}[2\log(2K)]^{-3/4} & \text{at asymmetric bifurcation point}, \\ \tfrac{2}{3}[2\log(2K)]^{-2/3} & \text{at unstable-symmetric bifurcation point}, \end{cases}$$

from the concrete forms of $f_\zeta(\zeta)$ given in eqns (15), (17) and (19). The limit distribution (27) is called the double exponential or the Gumbel distribution. Then, roughly speaking, ζ_K is of the order of c_K for large K, which we denote as

$$\zeta_K \sim c_K. \tag{28}$$

By means of eqns (4), (10), (25) and (26), we can rewrite eqn (28) for the minimum critical load $(\lambda_c)_K$ attained by K independent random imperfections as below:

$$(\lambda_c)_K \sim \lambda_c^0 + c_K C_0 \sigma^\rho =$$

$$\begin{cases} E_{\text{sample}}[\lambda_c] + c_K (\text{Var}_{\text{sample}}[\lambda_c])^{1/2} & \text{at limit point,} \\ E_{\text{sample}}[\lambda_c] + (2.35 + c_K/0.349)(\text{Var}_{\text{sample}}[\lambda_c])^{1/2} & \text{at asymmetric bifurcation point,} \\ E_{\text{sample}}[\lambda_c] + (1.861 + c_K/0.432)(\text{Var}_{\text{sample}}[\lambda_c])^{1/2} & \text{at unstable-symmetric bifurcation point,} \end{cases}$$

as $K \to +\infty$. We can use this equation to simulate $(\lambda_c)_K$ with reference to the sample mean $E_{\text{sample}}[\lambda_c]$ and the sample variance $\text{Var}_{\text{sample}}[\lambda_c]$. It should be emphasized here that these sample values may be based on a far smaller number of random imperfections than K. This shows the simplicity and the efficiency of the present method.

4. THEORY FOR DOUBLE CRITICAL POINTS

We are interested in the system (1) of nonlinear equilibrium equations of a structure with group symmetry, for which multiple critical points appear generically. Following Murota and Ikeda (1991, 1992) we assume that the symmetry of the equations is described mathematically by the equivariance of the equilibrium equations (1) to a finite group G, that is,

$$T(g)\mathbf{H}(\lambda, \mathbf{u}, \mathbf{v}) = \mathbf{H}(\lambda, T(g)\mathbf{u}, S(g)\mathbf{v}), \quad g \in G, \tag{29}$$

in terms of an $N \times N$ unitary matrix representation $T(g)$ of G on the N-dimensional space of the nodal displacement vector $\mathbf{u}$, and another $p \times p$ unitary representation $S(g)$ of G on the p-dimensional space of the imperfection parameter $\mathbf{v}$. Remember that any finite-dimensional representation is equivalent to a unitary representation.

We also assume that the displacement vector $\mathbf{u}_c^0$ at the critical point and the imperfection vector $\mathbf{v}^0$ for the perfect system are G-symmetric. That is, we assume

$$\Sigma(\mathbf{u}_c^0; G, T) = \Sigma(\mathbf{v}^0; G, S) = G,$$

where

$$\Sigma(\mathbf{u}; G, T) = \{g \in G | T(g)\mathbf{u} = \mathbf{u}\} \tag{30}$$

denotes the subgroup of G which expresses the symmetry of $\mathbf{u}$, and $\Sigma(\mathbf{v}; G, S)$ is defined similarly.

When the initial imperfection vector εd is subject to a normal distribution $N(\mathbf{o}, \varepsilon^2 W^{-1})$, we adopt an additional assumption on the compatibility of the variance-covariance matrix W^{-1} with the group symmetry:

$$S(g)WS(g)^{\text{T}} = W, \quad g \in G. \tag{31}$$

Note that this is satisfied if W is equal to the unit matrix I_p of order p, that is, each component of $\mathbf{d}$ is subject to the standard normal distribution.

Many dome and shell structures have regular-polygonal symmetry. To describe such symmetry, we henceforth assume G to be the dihedral group D_n of degree n defined by

$$D_n = \{e, r_n, \ldots, r_n^{n-1}, s, sr_n, \ldots, sr_n^{n-1}\} = \{r_n^k, sr_n^k \mid k = 0, 1, \ldots, n-1\}$$

with $r_n^n = s^2 = (sr_n)^2 = e$. Here e denotes the unit transformation, the element s stands for the reflection with respect to the XZ-plane, and r_n^k for the counter-clockwise rotation around the Z-axis at an angle of $2\pi k/n$ ($k = 1, \ldots, n-1$). Note that D_n indicates the invariance with respect to n rotations and n reflections.

Recall that the tangent stiffness (Jacobian) matrix of the perfect system is singular at the critical point $(\lambda_c^0, \mathbf{u}_c^0)$, i.e. eqn (2) holds for J^0. It follows from the D_n-equivariance (29)

that ker $((J^0)^T)$ is D_n-invariant, where ker $((J^0)^T)$ denotes the kernel of $(J^0)^T$, spanned by the critical eigenvectors ξ_i $(i = 1, \ldots, M)$. Critical points of a D_n-equivariant system are generically either simple $(M = 1)$ critical points or so-called group-theoretic double $(M = 2)$ points of bifurcation. In this paper a double point will mean a group-theoretic double point. This is a consequence of the fact that the irreducible representations of D_n are necessarily either one- or two-dimensional.

With a critical point, we associate a subgroup of D_n that represents the symmetry of the kernel of J^0, or of the vectors $\mathbf{u}$ belonging to ker (J^0). We denote this subgroup as

$$\Sigma (\ker (J^0)) = \Sigma (\ker (J^0) ; D_n, T) = \bigcap_{\mathbf{u} \in \ker (J^0)} \Sigma(\mathbf{u} ; D_n, T)$$

by extending the notation (30). Note that $\Sigma (\ker (J^0)) = \Sigma (\ker ((J^0)^T))$.

The explicit form of $\Sigma (\ker (J^0))$ is known from the group representation theory

$$\Sigma (\ker (J^0)) = \begin{cases} D_n & \text{at limit point,} \\ D_{n/2}, D_{n/2}^2 \text{ or } C_n & \text{at simple-symmetric point of bifurcation,} \\ C_m & \text{at double point of bifurcation,} \end{cases} \quad (32)$$

where m is a divisor of n; and

$$D_{n/2}^2 = \{r_n^{2k}, sr_n^{2k+1} \mid k = 0, 1, \ldots, n/2-1\} ;$$

$$C_m = \{r_n^{kn/m} \mid k = 0, 1, \ldots, m-1\}.$$

It will turn out that n/m is an important index characterizing a double critical point. The integer m in eqn (32) is to be determined in view of the symmetry of ker $((J^0)^T)$, that is, the symmetry of the critical eigenvector. In addition, we choose ξ_1 in such a way that $T(s)\xi_1 = \xi_1$.

4.1. Stochastic properties of the critical load

For group-theoretic double points of bifurcation, $C(\mathbf{d})$ and ρ in eqn (6) vary with the values of index n/m as follows [cf. Murota and Ikeda (1991)]

$$\begin{cases} \rho = 2/3, & C(\mathbf{d}) = -C_0 \cdot a^{2/3} & \text{if } n/m \geqslant 5 \text{ and unstable,} \\ \rho = 2/3, & C(\mathbf{d}) = C_0 \cdot a^{2/3} & \text{if } n/m \geqslant 5 \text{ and stable,} \\ \rho = 1/2, & C(\mathbf{d}) = -\tau(P B\mathbf{d}/\|P B\mathbf{d}\|)C_0 \cdot a^{1/2} & \text{if } n/m = 3, \\ \rho = 2/3, & C(\mathbf{d}) = -\tilde{\tau}(P B\mathbf{d}/\|P B\mathbf{d}\|)C_0 \cdot a^{2/3} & \text{if } n/m = 4, \end{cases} \quad (33)$$

where C_0 are (possibly different) positive constants; $\tau > 0$ and $\tilde{\tau}$ are nonlinear functions in $P B\mathbf{d}/\|P B\mathbf{d}\|$ (where $\|\cdot\|$ denotes the Euclidian norm); and

$$a = \|P B\mathbf{d}\|.$$

We decompose W as

$$W = V^T V$$

and define a transformation

$$\tilde{\mathbf{d}} = V\mathbf{d}. \quad (34)$$

This new variable $\tilde{\mathbf{d}}$ is subject to the standard normal distribution $N(\mathbf{o}, I_p)$.

As we have seen in eqn (33), the change $\tilde{\lambda}_c$ in the critical load is primarily governed by $a = \|P B\mathbf{d}\|$. It is proved in Section 4.2 of Murota and Ikeda (1992) that $\|P B\mathbf{d}\|^2$ can be expressed as

$$\| PB\mathbf{d} \|^2 = |\boldsymbol{\xi}_1^{\mathrm{T}} B\mathbf{d}|^2 + |\boldsymbol{\xi}_2^{\mathrm{T}} B\mathbf{d}|^2 = \tilde{\sigma}^2(|\boldsymbol{\eta}_1^{\mathrm{T}}\tilde{\mathbf{d}}|^2 + |\boldsymbol{\eta}_2^{\mathrm{T}}\tilde{\mathbf{d}}|^2) \tag{35}$$

with the use of the critical eigenvectors $\boldsymbol{\xi}_1$ and $\boldsymbol{\xi}_2$, $\tilde{\mathbf{d}} = V\mathbf{d}$ of eqn (34), mutually orthogonal p-dimensional unit vectors $\boldsymbol{\eta}_1$ and $\boldsymbol{\eta}_2$ which are independent of $\mathbf{d}$, and

$$\tilde{\sigma}^2 = \boldsymbol{\xi}_1^{\mathrm{T}} BW^{-1}B^{\mathrm{T}}\boldsymbol{\xi}_1 = \boldsymbol{\xi}_2^{\mathrm{T}} BW^{-1}B^{\mathrm{T}}\boldsymbol{\xi}_2.$$

Then, as is well known,

$$x = \left(\frac{a}{\tilde{\sigma}}\right)^2 \tag{36}$$

is subject to the exponential distribution, or the χ^2 distribution of two degrees of freedom. The probability density function of x is given as:

$$f_x(x) = \tfrac{1}{2}\exp\left(\frac{-x}{2}\right). \tag{37}$$

With the use of x of eqn (36) in eqn (33), we can introduce the normalized critical load increment as

$$\zeta = \frac{\tilde{\lambda}_c}{C_0\sigma^\rho} = \begin{cases} -x^{1/3} & \text{if } n/m \geqslant 5 \text{ and unstable } (\rho = 2/3), \\ x^{1/3} & \text{if } n/m \geqslant 5 \text{ and stable } (\rho = 2/3), \\ -\tau x^{1/4} & \text{if } n/m = 3(\rho = 1/2), \\ -\tilde{\tau}x^{1/3} & \text{if } n/m = 4(\rho = 2/3), \end{cases} \tag{38}$$

where $\sigma = \tilde{\sigma}\varepsilon$. As may be apparent from this equation, the explicit form of probability density function $f_\zeta(\zeta)$ of ζ depends entirely on the value of the index n/m.

4.1.1. *Case 1 : $n/m \geqslant 5$.* For an unstable-double point with $n/m \geqslant 5$, combining eqn (37) with eqn (38) leads to the probability density function $f_\zeta(\zeta)$, the reliability function $R_\zeta(\zeta)$, the expected value $E[\zeta]$, and the variance $\text{Var}[\zeta]$ of ζ:

$$f_\zeta(\zeta) = \frac{3\zeta^2}{2}\exp\left(\frac{-|\zeta|^3}{2}\right), \quad -\infty < \zeta < 0, \tag{39}$$

$$R_\zeta(\zeta) = 1 - \exp\left(\frac{-|\zeta|^3}{2}\right), \quad -\infty < \zeta < 0, \tag{40}$$

$$E[\zeta] = -2^{1/3}\Gamma\left(\frac{4}{3}\right) = -1.13,$$

$$E[\zeta^2] = 2^{2/3}\Gamma\left(\frac{5}{3}\right) = 1.43,$$

$$\text{Var}[\zeta] = 2^{2/3}\left\{\Gamma\left(\frac{5}{3}\right) - \left[\Gamma\left(\frac{4}{3}\right)\right]^2\right\} = (0.409)^2.$$
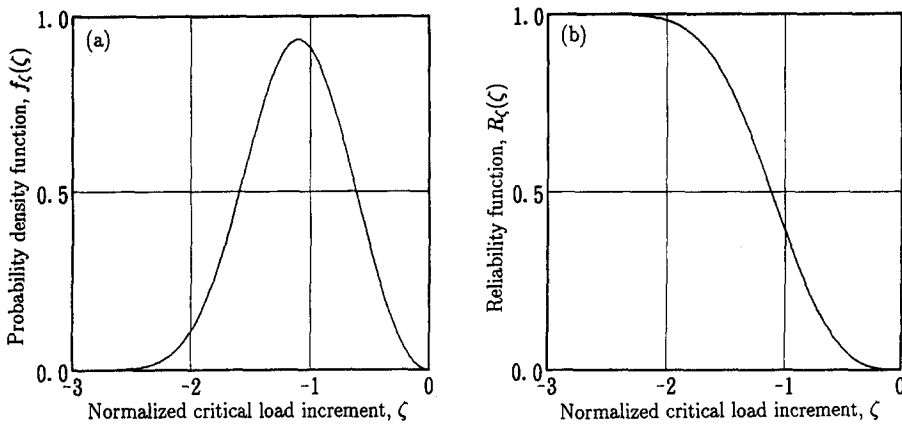
Fig. 2. Probability density function $f_\zeta(\zeta)$ and reliability function $R_\zeta(\zeta)$ of normalized critical load increment ζ for double critical points with $n/m \geqslant 5$. (a) Probability density function. (b) Reliability function.

Namely, $-\zeta$ is subject to the Weibull distribution. Figures 2(a) and (b) show the shape of the probability density function $f_\zeta(\zeta)$ and the reliability function $R_\zeta(\zeta)$ of $f_\zeta(\zeta)$, respectively. A simple calculation yields various statistical properties of the critical load λ_c as below:

$$f_{\lambda_c}(\lambda_c) = \frac{3(\lambda_c - \lambda_c^0)^2}{2C_0^3\sigma^2}\exp\left(\frac{-|\lambda_c - \lambda_c^0|^3}{2C_0^3\sigma^2}\right), \quad -\infty < \lambda_c < \lambda_c^0, \tag{41}$$

$$R_{\lambda_c}(\lambda_c) = 1 - \exp\left(\frac{-|\lambda_c - \lambda_c^0|^3}{2C_0^3\sigma^2}\right), \quad -\infty < \lambda_c < \lambda_c^0,$$

$$E[\lambda_c] = \lambda_c^0 - 2^{1/3}\Gamma\left(\frac{4}{3}\right)C_0\sigma^{2/3} = \lambda_c^0 - 1.13C_0\sigma^{2/3}, \tag{42}$$

$$\text{Var}[\lambda_c] = 2^{2/3}\left\{\Gamma\left(\frac{5}{3}\right) - \left[\Gamma\left(\frac{4}{3}\right)\right]^2\right\}C_0^2\sigma^{4/3} = (0.409C_0\sigma^{2/3})^2. \tag{43}$$

4.1.2. *Case 2 : $n/m = 3$.* As shown in eqn (38), ζ for $n/m = 3$ is given by

$$\zeta = -\tau(\psi)x^{1/4},$$

where it is known (Murota and Ikeda, 1991) that

$$\psi = \arg\left(\boldsymbol{\xi}_1^T \boldsymbol{B}\boldsymbol{d} + i\boldsymbol{\xi}_2^T \boldsymbol{B}\boldsymbol{d}\right) \tag{44}$$

(i denotes the imaginary unit) and $\tau(\psi) > 0$ is a solution to the equation

$$g(\tau) \equiv \frac{27}{256}\tau^6 - \frac{9}{8}\tau^2 - \frac{1}{\tau^2} = 2\cos(3\psi).$$

It is noteworthy that the variables $\tau(\psi)$ and $x^{1/4}$ are statistically independent. The probability density function of $b \equiv (a/\tilde{\sigma})^{1/2} = x^{1/4}$ is computed with reference to eqn (37)

as

$$f_b(b) = 2b^3 \exp\left(\frac{-b^4}{2}\right), \quad 0 < b < \infty.$$

The mean and variance of b are evaluated to be

$$E[b] = 2^{1/4}\Gamma\left(\frac{5}{4}\right) = 1.08,$$

$$\text{Var}[b] = \sqrt{\frac{\pi}{2}} - \sqrt{2}\left[\Gamma\left(\frac{5}{4}\right)\right]^2 = (0.302)^2.$$

On the other hand, on noting that ψ of eqn (44) is uniformly distributed in the range $0 < \psi < 2\pi$, we can arrive at the probability density function of τ as follows:

$$f_\tau(\tau) = \frac{1}{2\pi}\frac{d\psi}{d\tau} = \frac{1}{2\pi}\cdot\frac{g'(\tau)}{\sqrt{1-g(\tau)^2/4}}, \quad \tau_{\min} < \tau < \tau_{\max},$$

with

$$\tau_{\min} = \frac{2}{\sqrt{3}}, \quad \tau_{\max} = 2.$$

The density functions $f_\tau(\tau)$ and $f_b(b)$ are depicted in Figs 3(a) and (b). By numerical integration we obtain

$$E[\tau] = 1.77, \quad \text{Var}[\tau] = (0.221)^2.$$

It should be noted that τ lies in a bounded positive interval away from zero, and therefore plays only a secondary role compared with b.

Then the probability density function $f_\zeta(\zeta)$ of the normalized critical load increment
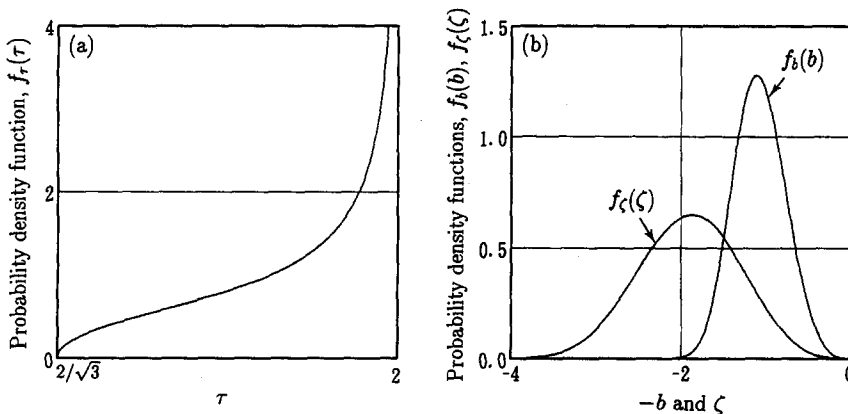
$$\zeta = -b\tau$$

is given by

Fig. 3. Probability density functions of normalized critical load increment ζ for double critical points with $n/m = 3$. (a) $f_\tau(\tau)$. (b) $f_b(b)$ and $f_\zeta(\zeta)$.

$$f_\zeta(\zeta) = \int_{\tau_{\min}}^{\tau_{\max}} f_b\left(\frac{|\zeta|}{\tau}\right)\frac{f_\tau(\tau)}{\tau}\,d\tau, \quad -\infty < \zeta < 0. \tag{45}$$

This shows that the probability density function of ζ is independent of individual structures, just as in Case 1. A numerical integration yields

$$E[\zeta] = 1.91, \qquad\qquad \text{Var}[\zeta] = (0.590)^2,$$

$$E[\lambda_c] = \lambda_c^0 - 1.91 C_0\sigma^{1/2}, \quad \text{Var}[\lambda_c] = (0.590 C_0\sigma^{1/2})^2. \tag{46}$$

4.1.3. *Case 3 : $n/m = 4$.* As shown in eqn (38), ζ for $n/m = 4$ is given by

$$\zeta = -\tilde{\tau}(\psi)x^{1/3},$$

where

$$\psi = \arg(\xi_1^T B\mathbf{d} + i\xi_2^T B\mathbf{d})$$

and $\tilde{\tau}(\psi)$ is a solution to an algebraic equation, which varies with individual structures [see Murota and Ikeda (1991) for details]. We normalize $\tilde{\tau}(\psi)$ in such a manner that its maximum $\tilde{\tau}_{\max}$ is equal to unity.

As in the case of $n/m = 3$, the variables $\tilde{\tau}(\psi)$ and $b = x^{1/3}$ are statistically independent. The distribution of b coincides with the one described in eqn (39). The probability distribution of $\tilde{\tau}$, and hence that of ζ, vary with individual structures.

If necessary, the probability distribution of ζ may be empirically evaluated as follows. First compute $\tilde{\lambda}_c$ for the imperfection modes

$$\mathbf{d}^*(\varphi) = \cos\varphi\,\frac{B^T\xi_1}{\|B^T\xi_1\|} + \sin\varphi\,\frac{B^T\xi_2}{\|B^T\xi_2\|}$$

for sufficiently many values of φ $(0 \leqslant \varphi < 2\pi)$. Since $\|PB\mathbf{d}^*(\varphi)\|$ is independent of φ, this gives the distribution of $\tilde{\tau}$. Then the distribution of ζ is computed from the formula (45).

The values of average $E[\zeta]$ and variance Var $[\zeta]$, which vary with individual structures, must be obtained through numerical integration for each case. For the theoretical evaluation, the value of C_0 is evaluated from eqn (38) for φ_0 that maximizes $|\tilde{\lambda}_c|$, and hence with $\tilde{\tau}(\varphi_0) = \tilde{\tau}_{\max} = 1$.

4.2. Evaluation of probability density function

As explained in Section 4.1 the theoretical evaluation is also applicable to double critical points. The form of the probability density function $f_\zeta(\zeta)$ is unique for $n/m \neq 4$, but is dependent on individual structures for $n/m = 4$. Its form is explicitly given for $n/m \geqslant 5$, whereas numerical integration by eqn (45) is needed for $n/m = 3$ and 4.

The semi-empirical evaluation similar to the one explained in Section 3.3 is also applicable for double critical points. For $n/m \neq 4$ the critical load λ_c^0 for the perfect system and the variable $C_0\sigma^\rho$, which determines the semi-empirical probability density function of load increment $\tilde{\lambda}_c$ by eqn (41), are computed from eqns (42), (43) and (46) as

$$C_0\sigma^\rho = \begin{cases} (\text{Var}_{\text{sample}}[\lambda_c])^{1/2}/0.409, & n/m \geqslant 5(\rho = 2/3), \\ (\text{Var}_{\text{sample}}[\lambda_c])^{1/2}/0.590, & n/m = 3(\rho = 1/2), \end{cases}$$

$$\lambda_c^0 = \begin{cases} E_{\text{sample}}[\lambda_c] + 2.75\,(\text{Var}_{\text{sample}}[\lambda_c])^{1/2}, & n/m \geqslant 5, \\ E_{\text{sample}}[\lambda_c] + 3.24\,(\text{Var}_{\text{sample}}[\lambda_c])^{1/2}, & n/m = 3. \end{cases}$$

For $n/m = 4$, instead, the values of $E[\lambda_c]$ and Var $[\lambda_c]$ obtained though numerical integration yield the values of $C_0\sigma^\rho$ and λ_c^0. It should be noted that the imperfection sensitivity matrix B is needed for this case.

4.3. Distribution of minimum values

For double critical points with $n/m \neq 4$, the asymptotic formula (27) for the minimum load ζ_K achieved by K independent random imperfections also holds with

$$c_K = \begin{cases} -[2\log K]^{1/3} & \text{if } n/m \geq 5, \\ -[2\log K]^{1/4} & \text{if } n/m = 3, \end{cases}$$

$$d_K = \begin{cases} \frac{2}{3}[2\log K]^{-2/3} & \text{if } n/m \geq 5, \\ \frac{1}{2}[2\log K]^{-3/4} & \text{if } n/m = 3. \end{cases}$$

For $n/m \geq 5$, with reference to eqn (39), the probability distribution function of ζ_K is expressed as

$$F_K(\zeta_K) = 1 - \left[1 - \exp\left(\frac{-|\zeta_K|^3}{2}\right) \right]^K, \quad -\infty < \zeta_K < 0 \tag{47}$$

and the differentiation of eqn (47) gives its probability density function

$$f_K(\zeta_K) = \frac{3K\zeta_K^2}{2} \exp\left(\frac{-|\zeta_K|^3}{2}\right) \left[1 - \exp\left(\frac{-|\zeta_K|^3}{2}\right) \right]^{K-1},$$

the shape of which is plotted in Fig. 4 for various values of K. The peak of this function shifts toward $-\infty$ and becomes sharper in association with the increase in K.

5. EXAMPLES

5.1. Asymmetric simple bifurcation point

Consider the propped cantilever of Fig. 5 comprising a truss member, simply supported with a rigid foundation at node 1 and supported by horizontal and vertical springs at node 2. A vertical load λ is applied to the free node 2. This cantilever has also been put to use in Ikeda and Murota (1990a, 1991) as an example for an asymmetric simple bifurcation point.

The system of equilibrium equations is

$$\mathbf{H}(\lambda, \mathbf{u}, \mathbf{v}) \equiv EA\left(\frac{1}{L} - \frac{1}{\tilde{L}}\right)\begin{pmatrix} x - x_1 \\ y - y_1 \end{pmatrix} + \begin{pmatrix} F_{sx} \\ F_{sy} \end{pmatrix} - \begin{pmatrix} 0 \\ \lambda \end{pmatrix} = \mathbf{o}, \tag{48}$$
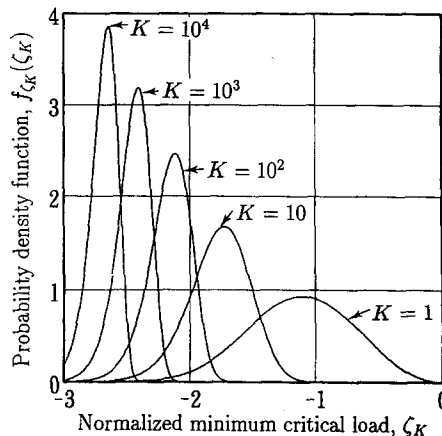
where

Fig. 4. Probability density functions of the minimum critical load ζ_K attained by K independent random imperfections for double critical points with $n/m \geq 5$ ($K = 1, 10, 10^2, 10^3, 10^4$).
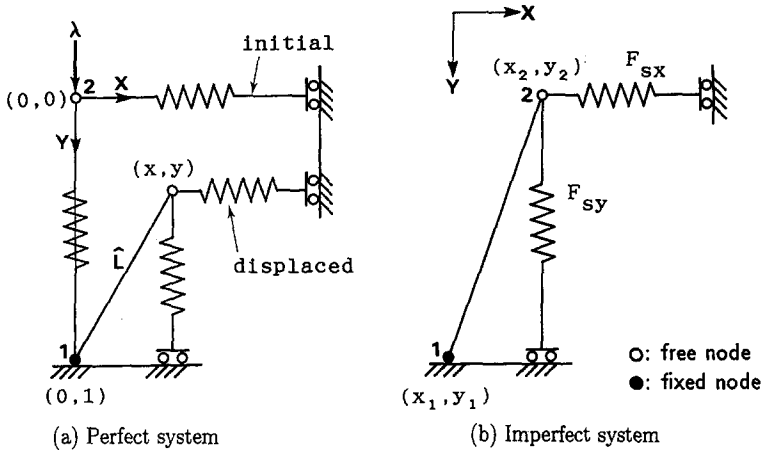
Fig. 5. Propped cantilever. (a) Perfect system. (b) Imperfect system.

$$L = [(x_2-x_1)^2+(y_2-y_1)^2]^{1/2}, \quad \hat{L} = [(x-x_1)^2+(y-y_1)^2]^{1/2},$$

$$F_{sx} = EA\left[\frac{x-x_2}{L}+\left(\frac{x-x_2}{L}\right)^2\right], \quad F_{sy} = EA\frac{y-y_2}{L}.$$

$\mathbf{u} = (x, y)^T$ is the location of node 2 after displacement, (x_i, y_i) is the initial location of node i ($i = 1, 2$), and F_{sx} and F_{sy} are the horizontal and vertical forces exerted by the springs, respectively; E is the modulus of elasticity and A is the cross-section.

The equilibrium paths for the perfect cantilever expressed by eqns (48) consists of a main path and a pair of bifurcation paths branching at an asymmetric simple bifurcation point. The critical eigenvector at this point is $\boldsymbol{\xi} = (1, 0)^T$ and $(\lambda_c^0, x_c^0, y_c^0) = (EA, 0, 1/2)$.

We choose (x_i, y_i) ($i = 1, 2$) as imperfection parameters, and define

$$\mathbf{v} = (x_1, y_1, x_2, y_2)^T$$

as an imperfection parameter vector. In the perfect case, we have

$$\mathbf{v}^0 = (0, 1, 0, 0)^T.$$

We assume that

$$\varepsilon\mathbf{d} = \mathbf{v} - \mathbf{v}^0$$

is subject to a multivariate normal distribution $N(\mathbf{o}, \varepsilon^2 I_4)$, that is

$$W^{-1} = I_4. \tag{49}$$

First, following the theoretical evaluation, we obtain the probability density function of critical load. The imperfection sensitivity matrix

$$B = EA\begin{pmatrix} 1 & 0 & -1 & 0 \\ 0 & -2 & 0 & 0 \end{pmatrix} \tag{50}$$

is obtained by differentiating $\mathbf{H}$ in eqns (48) with respect to $\mathbf{v}$ and evaluating at the bifurcation point [cf. eqn (5)]. Use of eqns (49) and (50) in eqn (11) leads to
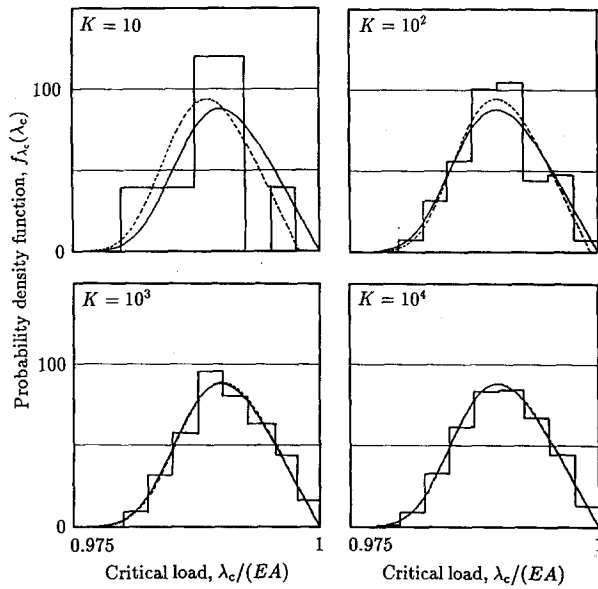
Fig. 6. The influence of the sample size K on the semi-empirical probability density function and the histogram (10^5 samples; $\varepsilon = 10^{-4}$) for the propped cantilever (asymmetric simple bifurcation point). Solid curve: theoretical probability density function; dashed curve: semi-empirical probability density function; histogram: numerical experiment.

$$\sigma^2 = \varepsilon^2 \boldsymbol{\xi}^T B W^{-1} B^T \boldsymbol{\xi} = 2\varepsilon^2.$$

Further, we solved eqns (48) for an arbitrarily chosen imperfection mode $\mathbf{d} = (1, 1, -1, -1)^T$ and $\varepsilon = 10^{-6}$, which is sufficiently small as to make the asymptotic formula (6) accurate, to arrive at

$$\tilde{\lambda}_c = 0.00141 EA \sim C_0(\boldsymbol{\xi}^T B\mathbf{d})^{1/2}\varepsilon^{1/2} = \sqrt{2} \times 10^{-3} C_0$$

by eqns (6) and (7). The solution of this asymptotic relationship yields

$$C_0 \sim 1.0 EA.$$

Based on the values of C_0 and σ^2 evaluated in this manner, we computed from eqn (21) the theoretical probability density function $f_{\lambda_c}(\lambda_c)$ of the critical load λ_c shown by the solid line in Fig. 6.

Next, following the semi-empirical evaluation, which does not necessitate the computation of B in eqn (5), we have randomly chosen $K = 10^5$ imperfection modes subject to the aforementioned normal distribution $N(\mathbf{o}, \varepsilon^2 I_4)$ for $\varepsilon\mathbf{d}$ and computed a set of critical loads λ_c for a constant imperfection magnitude $\varepsilon = 10^{-2}$, 10^{-3} and 10^{-4}. Table 1 lists the sample mean $E_{\text{sample}}[\lambda_c]$ and the sample standard deviation $(\text{Var}_{\text{sample}}[\lambda_c])^{1/2}$ of these critical loads. From eqns (25) and (26), we have empirically evaluated the values of λ_c^0 and $C_0\sigma^{1/2}$ also listed in this table. In association with the decrease of imperfection magnitude ε, the evaluated values converge to the exact values, in agreement with the asymptotic nature of eqn (6). The semi-empirical evaluation seems to be quite accurate.

Table 1. Evaluated values of λ_c^0 and $C_0\sigma^{1/2}$ ($K = 10^5$)

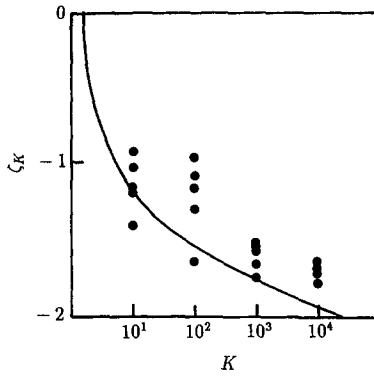|	$E_{\text{sample}}[\lambda_c]$	$(\text{Var}_{\text{sample}}[\lambda_c])^{1/2}$	λ_c^0	$C_0\sigma^{1/2}$	$C_0(\sigma/\varepsilon)^{1/2}$
10^{-2}	0.905	3.87×10^{-2}	0.9964	1.11×10^{-1}	1.11
$\varepsilon = 10^{-3}$	0.969	1.30×10^{-2}	0.9999	3.73×10^{-2}	1.18
10^{-4}	0.990	4.15×10^{-3}	1.0000	1.19×10^{-2}	1.19
Exact values			1.0000		1.19

Fig. 7. Comparison of ζ_K and theoretical estimation (28) plotted against K in a semi-logarithmic scale for an asymmetric simple bifurcation point ($\varepsilon = 10^{-6}$). ($\bullet$) : empirical ζ_K; solid line : theoretical estimation (28).

In order to see the improvement in the semi-empirical probability density function and the histogram in association with the increase in the sample size K of random initial imperfections, they are plotted in Fig. 6 based on the first $K = 10$, 10^2, 10^3 and 10^4 random samples for $\varepsilon = 10^{-4}$. Although the improvement of the histogram seems to be slow, the semi-empirical probability density functions (shown by the dashed lines) quickly approach the theoretical one (the solid line). This implies the importance of the knowledge of the explicit form of the probability density function, and hence of the present method.

We plotted in Fig. 7 for $\varepsilon = 10^{-6}$ the comparison of the empirical minimum load ζ_K achieved by K random imperfections [shown by the symbols ($\bullet$)] and its theoretical evaluation by eqn (28) (shown by the solid line). This evaluation is fairly consistent with the empirical ζ_K.

5.2. Limit point and unstable-symmetric simple bifurcation point

We consider the regular octagonal truss dome in Fig. 8(a) as a numerical example for a limit point and the hexagonal one in (b) for an unstable-symmetric simple point of

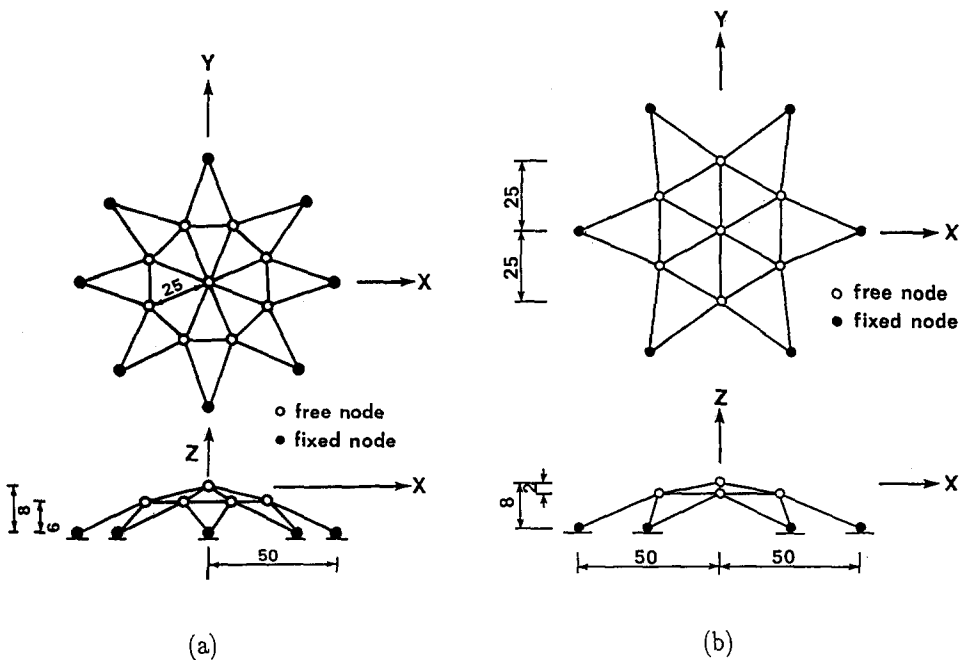(a)   (b)

Fig. 8. (a) Regular-octagonal truss dome (limit point). (b) Regular-hexagonal truss dome (unstable-symmetric simple bifurcation point).

bifurcation. All members of these domes have the same modulus of elasticity E and the same cross-section A. Uniform vertical loads λ are applied to each free node for the former dome (a) ; and vertical loads applied 0.5λ to the crown node and λ to other free nodes for the latter (b). We have carried out a finite displacement analysis to solve equilibrium equations (1) to note that the first critical load for the former is governed by a limit point and for the latter by an unstable-symmetric simple bifurcation point.

We choose the initial location (x_i, y_i, z_i) $(i = 1, \ldots, k)$ of nodes as imperfection parameters ($k = 17$ for the former and $k = 13$ for the latter). The imperfection vector is subject to a normal distribution $N(\mathbf{0}, \varepsilon^2 I_{3k})$ with $\varepsilon = 10^{-3}$. We utilized the explicit form of the imperfection sensitivity matrix B for these imperfection variables given in Ikeda and Murota (1990b). Equation (11) yields

$$\sigma^2 = \begin{cases} 2.77 \times 10^{-13}(EA)^2, & \text{at limit point,} \\ 3.49 \times 10^{-12}(EA)^2, & \text{at unstable-symmetric simple bifurcation point,} \end{cases}$$

and eqn (6) gives

$$C_0 = \begin{cases} 1.28, & \text{at limit point,} \\ 0.051(EA)^{1/3}, & \text{at unstable-symmetric simple bifurcation point,} \end{cases}$$

where the values of $B^T\xi$ computed at the relevant critical point are used herein. The use of these values in eqns (15) and (19) leads to the theoretical probability density function of ζ shown as the solid lines in Fig. 9.
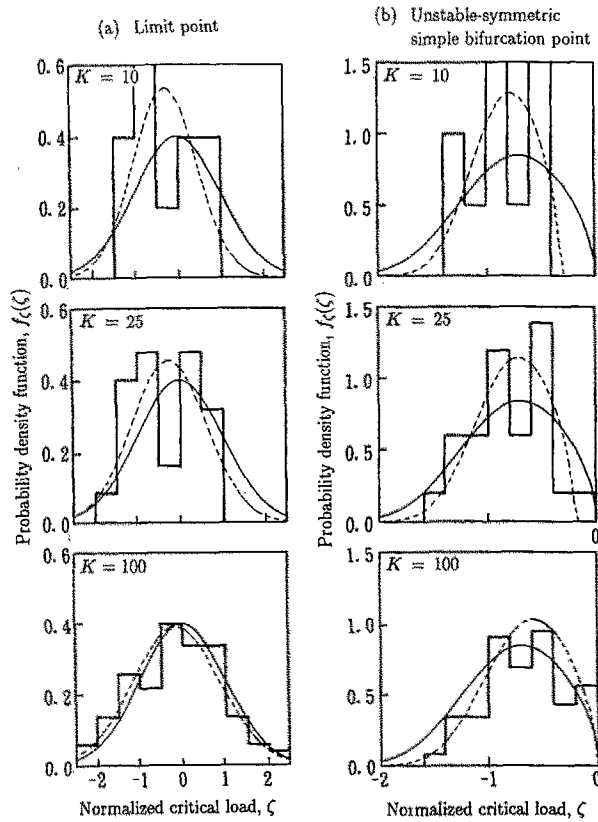

Fig. 9. Comparison of theoretical and semi-empirical probability density function $f_\zeta(\zeta)$ and empirical histogram of normalized critical load increment ζ ($\varepsilon = 10^{-3}$). (a) Limit point (regular-octagonal truss dome). (b) Unstable-symmetric simple bifurcation point (regular-hexagonal truss dome). Solid curve : theoretical probability density function ; dashed curve : semi-empirical probability density function ; histogram : numerical experiment.

Table 2. Evaluated values of λ_c^0 and $C_0\sigma^\rho$ ($\varepsilon = 10^{-3}$)
(a) Limit point

	$\lambda_c^0 = E_{sample}[\lambda_c]$	$C_0\sigma = (Var_{sample}[\lambda_c])^{1/2}$
10	3.746×10^{-4}	5.02×10^{-7}
$K = $ 25	3.747×10^{-4}	5.91×10^{-7}
100	3.747×10^{-4}	6.88×10^{-7}
Exact values	3.748×10^{-4}	6.74×10^{-7}

(b) Unstable-symmetric simple bifurcation point

	$E_{sample}[\lambda_c]$	$(Var_{sample}[\lambda_c])^{1/2}$	λ_c^0	$C_0\sigma^{2/3}$
10	7.635×10^{-4}	2.20×10^{-6}	7.68×10^{-4}	5.09×10^{-6}
$K = $ 25	7.639×10^{-4}	2.46×10^{-6}	7.69×10^{-4}	5.68×10^{-6}
100	7.648×10^{-4}	2.76×10^{-6}	7.70×10^{-4}	6.37×10^{-6}
Exact values	7.638×10^{-4}	3.35×10^{-6}	7.70×10^{-4}	7.74×10^{-6}

For each dome, we have randomly chosen $K = 10$, 25 and 100 samples of εd subject to $N(\mathbf{0}, \varepsilon^2 I_{3k})$, and traced the equilibrium paths to compute the normalized critical load increment ζ. Table 2 lists the improvement of the semi-empirical evaluation of λ_c^0 and $C_0\sigma^\rho$ by eqns (25) and (26). The histogram, the theoretical and the semi-empirical probability density functions $f_\zeta(\zeta)$ are compared in Fig. 9(a) for a limit point and in (b) for an unstable-symmetric simple point of bifurcation. The theoretical and the semi-empirical curves are in relatively good agreement with the observed histogram for each case.

5.3. Double critical (bifurcation) points

As numerical examples for double critical points we consider elastic n-bar truss tents ($n = 3$, 4, 5) shown in Fig. 10, and regular n-gonal truss domes ($n = 3$, 4, 5) in Fig. 11 [these examples were also employed in Murota and Ikeda (1992)]. The truss tents are subject to a vertical load λ applied to the top node, the truss domes to uniform vertical loads λ applied to each free node except for the center node. All members of these structures have the same modulus of elasticity E and the same cross-section A for the perfect case. Such symmetric stiffness distribution, accompanied by symmetries in geometry and loading, will result in the group-equivariance (29) of the equilibrium equations of these truss structures. Accordingly, the equations of n-bar truss tents ($n = 3$, 4, 5) and also those of regular n-gonal truss domes ($n = 3$, 4, 5) are D_n-equivariant.

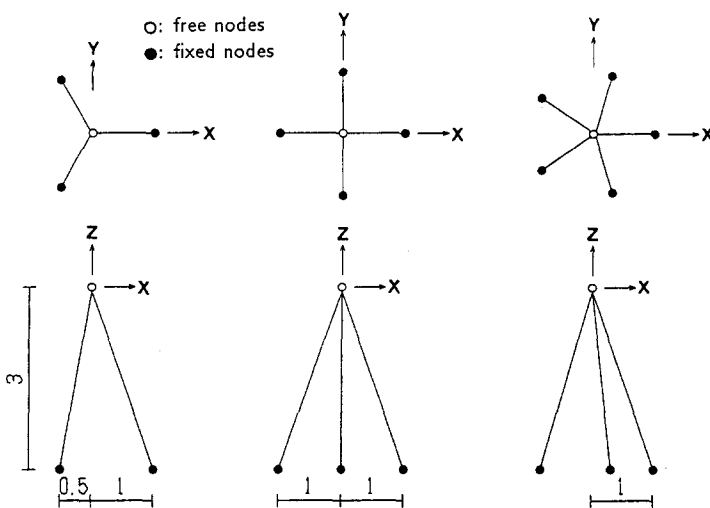We define an imperfection parameter vector as

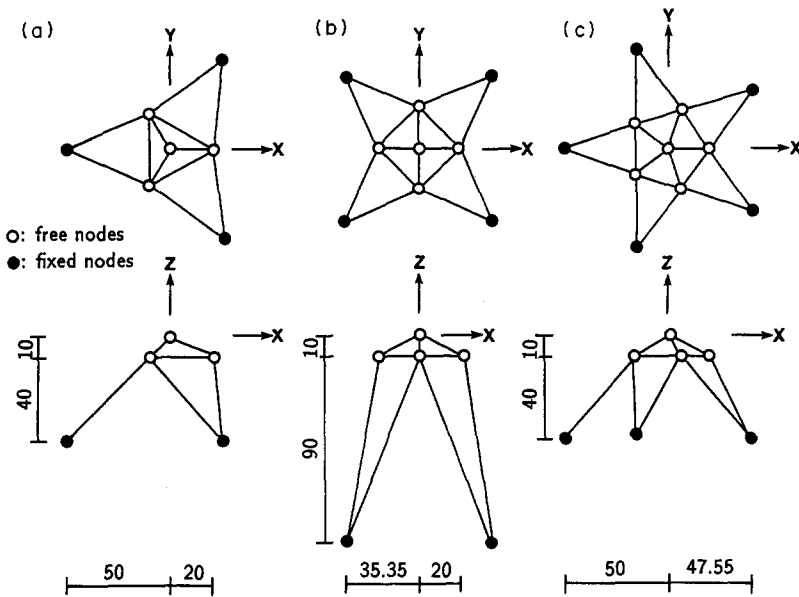
Fig. 10. n-bar truss tents ($n = 3, 4, 5$).

Fig. 11. Regular n-gonal truss domes (n = 3, 4, 5). (a) Triangular. (b) Square. (c) Pentagonal.

$$\mathbf{v} = (A_1, \ldots, A_p)^{\mathrm{T}},$$

where A_i ($i = 1, \ldots, p$) are the cross-sections of the ith members. For the perfect structure, we have

$$\mathbf{v}^0 = (A, \ldots, A)^{\mathrm{T}}.$$

We assume that $\varepsilon\mathbf{d} = \mathbf{v} - \mathbf{v}^0$ is subject to a multivariate normal distribution $N(\mathbf{o}, \varepsilon^2 I_p)$. Then the group symmetry (31) of W is satisfied.

The finite displacement analysis of these trusses for the perfect cases ($\varepsilon = 0$) was performed to note that their critical loads are governed by unstable group-theoretic double points of bifurcation, with C_1-symmetric kernel space ker $((J^0)^{\mathrm{T}})$ with $m = 1$. These double points for $n = 3$, 4 and 5 correspond to the three cases $n/m = 3$, 4 and 5 in Section 4, respectively.

For each truss structure, we have randomly chosen $K = 100$ imperfection modes of $\varepsilon\mathbf{d} = \mathbf{v} - \mathbf{v}^0$ subject to a multivariate normal distribution $N(\mathbf{o}, \varepsilon^2 I_p)$ and computed a set of critical loads ζ for a constant imperfection magnitude $\varepsilon = 10^{-4}$. Then λ_c^0 and $C_0\sigma^\rho$ are computed based on the theoretical and empirical evaluation techniques. The empirical histogram obtained from these 100 imperfections and the theoretical (for $n/m \neq 4$) and semi-empirical probability density function $f_\zeta(\zeta)$ are compared in Figs 12, 13 and 14 for
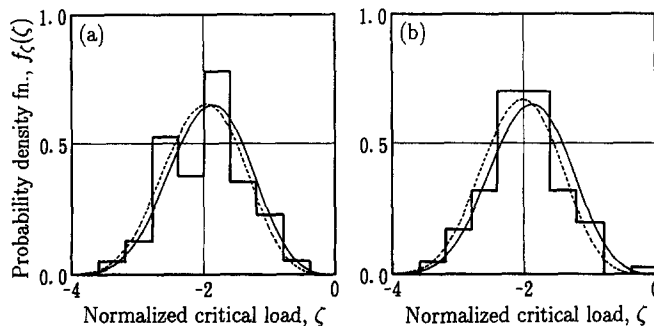

Fig. 12. Comparison of probability density function $f_\zeta(\zeta)$ and empirical histogram (100 samples) at an unstable double point of bifurcation ($n/m = 3$). (a) 3-bar truss. (b) 3-gonal truss dome. Solid curve: theoretical probability density function; dashed curve: semi-empirical probability density function; histogram: numerical experiment.
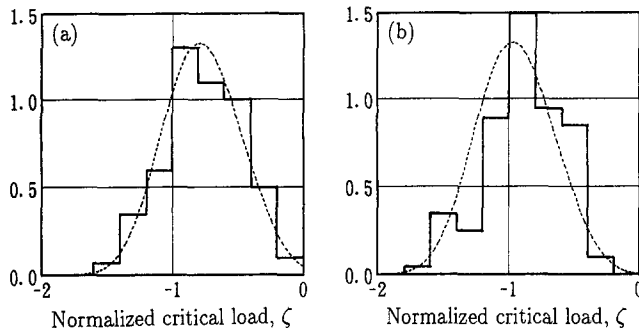
Fig. 13. Comparison of probability density function $f_\zeta(\zeta)$ and empirical histogram (100 samples) at an unstable double point of bifurcation ($n/m = 4$). (a) 4-bar truss. (b) 4-gonal truss dome. Dashed curve: semi-empirical probability density function; histogram: numerical experiment.
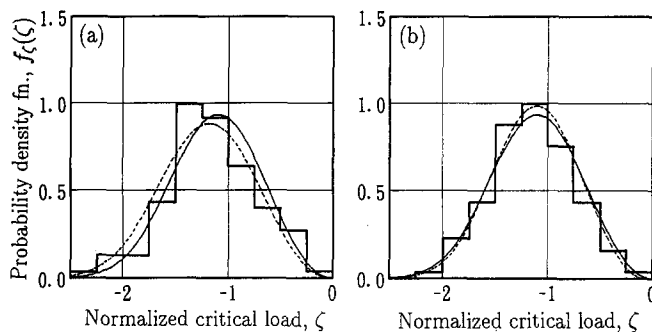

Fig. 14. Comparison of probability density function $f_\zeta(\zeta)$ and empirical histogram (100 samples) at an unstable double point of bifurcation ($n/m = 5$). (a) 5-bar truss. (b) 5-gonal truss dome. Solid curve: theoretical probability density function; dashed curve: semi-empirical probability density function; histogram: numerical experiment.

$n/m = 3$, 4 and 5, respectively. The theoretical values of $C_0 \sigma^\rho$ were used to normalize ζ for $n/m \neq 4$. The theoretical and empirical functions are in fair agreement with the histogram in each case. This shows the validity of the present method.

6. CONCLUSION

In this paper we have made a theoretical study on random initial imperfections of (symmetric) structures to arrive at various kinds of stochastic properties of critical loads. As we have seen in Figs 1 and 2, the probability density function for a limit point agrees with the normal distribution, but those for the bifurcation points do not. This raises a question on the validity of the simplifying assumption often utilized in the first-order, second-moment method that critical loads are normally distributed (Arbocz and Hol, 1991). Put otherwise, this shows the importance of the present method that can derive the explicit form of probability density function by virtue of the asymptoticity assumption. Of course the use of this assumption make the results less accurate, especially when imperfections are large, in comparison with the former method that solves the governing nonlinear equations to obtain critical loads. The tradeoff between these two methods will require further studies.

The theoretical method presented in this paper is readily applicable to truss structures, for which the explicit forms of the matrix B have already been obtained in Ikeda and Murota (1990b). It will be the natural course of future research to extend the theoretical method to other structures by deriving the explicit form of the matrix for each structure. It is to be emphasized here that the present formulation regarding D_n-equivariant structures can be extended to those with other types of symmetries in a straightforward manner, when the asymptotic behavior of the critical load depends solely on $a = \| PB\mathbf{d} \|$.

REFERENCES

Arbocz, J. and Hol, J. M. A. M. (1991). Collapse of axially compressed cylindrical shells with random imperfections. *AIAA Jl* **29**(12), 2247–2256.

Astill, J., Nosseir, C. J. and Shinozuka, M. (1972). Impact loading on structures with random properties. *J. Struct. Mech.* **1**(1), 63–67.

Baecher, G. B. and Ingra, T. S. (1981). Stochastic FEM in settlement predictions. *J. Geotech. Engng Div.* **107**(4), 449–463.

Bolotin, V. V. (1958). Statistical methods in the nonlinear theory of elastic shells. Izvestija Academii Nauk SSSR. Otdeleni Tekhnicheskikh Nauk 3 (English translation, NASA TTF-85, 1962, 1–16).

Dinkevich, S. (1991). Finite symmetric systems and their analysis. *Int. J. Solids Structures* **27**(10), 1215–1253.

Elishakoff, I. (1979). Buckling of a stochastically imperfect finite column on a nonlinear elastic foundation. *J. Appl. Mech.* **46**(2), 411–416.

Elishakoff, I. (1983). *Probabilistic Methods in the Theory of Structures*. Wiley, New York.

Elishakoff, I. and Arbocz, J. (1982). Reliability of axially compressed cylindrical shells with random axisymmetric imperfections. *Int. J. Solids Structures* **18**, 563–585.

Elishakoff, I., van Manen, S., Vermeulen, P. G. and Arbocz, J. (1987). First-order second-moment analysis of the buckling of shells with random initial imperfections. *AIAA Jl* **25**(8), 1113–1117.

Galambos, J. (1978). *The Asymptotic Theory of Extreme Order Statistics*. Wiley, New York.

Golubitsky, M. and Schaeffer, D. G. (1985). *Singularities and Groups in Bifurcation Theory. Vol. 1*. Springer, Berlin.

Golubitsky, M., Stewart, I. and Schaeffer, D. G. (1988). *Singularities and Groups in Bifurcation Theory. Vol. 2*. Springer, Berlin.

Healey, T. J. (1988). A group theoretic approach to computational bifurcation problems with symmetry. *Comput. Meth. Appl. Mech. Engng* **67**, 257–296.

Ikeda, K. and Murota, K. (1990a). Critical initial imperfection of structures. *Int. J. Solids Structures* **26**(8), 865–886.

Ikeda, K. and Murota, K. (1990b). Computation of critical initial imperfection of truss structures. *J. Engng Mech. Div. ASCE* **116**(10), 2101–2117.

Ikeda, K. and Murota, K. (1991). Random initial imperfections of structures. *Int. J. Solids Structures* **28**(8), 1003–1021.

Ikeda, K., Murota, K. and Fujii, H. (1991). Bifurcation hierarchy of symmetric structures. *Int. J. Solids Structures* **27**(12), 1551–1573.

Karadeniz, H. van Manen, S. and Vrouwenvelder, A. (1982). Probabilistic reliability analysis for the fatigue limit state of gravity and jacket type structures. *Proc. Third Int. Conf.-BOSS*. McGraw-Hill, London, 147–165.

Kendall, K. and Stuart, A. (1977). *The Advanced Theory of Statistics. Vol. 1* (4th Edn). Charles Griffin, London.

Kirkpatrick, S. W. and Holmes, B. S. (1989). Effects of initial imperfections on dynamic buckling of shells. *J. Engng Mech. Div. ASCE* **115**(5), 1075–1093.

Koiter, W. T. (1945). On the stability of elastic equilibrium. Dissertation. Delft, Holland (English translation: NASA Tech. Trans. F10: 833, 1967).

Lindberg, H. E. (1988). Random imperfections for dynamic pulse buckling. *J. Engng Mech. Div. ASCE* **114**(7), 1144–1165.

Murota, K. and Ikeda, K. (1991). Critical imperfection of symmetric structures. *SIAM J. Appl. Math.* **51**(5), 1222–1254.

Murota, K. and Ikeda, K. (1992). On random imperfection for structures of regular-polygonal symmetry. *SIAM J. Appl. Math.* **52**(6), 1780–1803.

Roorda, J. and Hansen, J. S. (1972). Random buckling behavior in axially loaded cylindrical shells with axisymmetric imperfections. *J. Spacecraft* **9**(2), 88–91.

Sattinger, D. H. (1979). *Group Theoretic Methods in Bifurcation Theory. Lecture Notes in Mathematics 762*. Springer, Berlin.